Journal of Polymers and the Environment (2022) 30:258–269
https://doi.org/10.1007/s10924-021-02195-2

ORIGINAL PAPER

Orange Juice Processing Waste as a Biopolymer Base for Biodegradable Film Formation Reinforced with Cellulose Nanofiber and Activated with Nettle Essential Oil

Seyedeh Elham Mousavi Kalajahi[1] · Ainaz Alizadeh[1] · Hamed Hamishehkar[2] · Hadi Almasi[3] · Narmela Asefi[1]

Accepted: 25 May 2021 / Published online: 2 June 2021

Abstract
Concerns about environmental problems have led to the development of biodegradable packaging. Food wastes as a byproduct could be a good source for biopolymers. This study aimed to describe the physical and antimicrobial features of nano biocomposite films based on orange waste powder (OWP) with different concentrations of nettle essential oil (NEO) (1.5 and 3%) as an antibacterial agent and cellulose nanofiber (CNF) (3 and 6%) as a structural reinforcement. Thus, Field emission scanning electron microscopy (FE-SEM), Fourier-transform infrared spectroscopy (FTIR), X-ray diffraction (XRD), and differential scanning calorimetry analysis (DSC) were performed. Further, tensile strength, elongation at break, water vapor permeability, and antimicrobial properties were investigated. As a result, the addition of CNF improved the tensile strength and water barrier properties of the samples. Compared to the control film, adding NEO (3%) decreased the tensile strength but increased water vapor permeability and melting temperature. Moreover, the OWP-based film samples had an antimicrobial effect against five foodborne pathogens; this effect was increased considerably by enhancing the NEO concentration. In this regard, the maximum and minimum susceptibility was related to the *Staphylococcus aureus* and *Salmonella enterica*, respectively. In conclusion, orange waste could be used to produce an active film with improved physicomechanical and antibacterial properties by incorporating CNF and NEO.

Keywords Cellulose nanofiber · Nano biocomposite film · Nettle essential oil · Orange waste

Introduction

Food packaging materials are almost petroleum-based plastics widely used due to their availability, low price, and desirable properties. However, such plastics cause many environmental problems due to their non-biodegradability [1, 2]. Furthermore, the migration of some compounds, such as plasticizers, monomers, and solvent residues, from plastics into the food leads to off-flavor and, thus reducing food safety [3]. Concerns about the health problems related to plastics and consumer's demand for high-quality food products have led to the development of biodegradable packaging materials such as films and coatings [4]. In recent years, various biopolymers, including proteins and polysaccharides, have been used to develop biodegradable films to replace synthetic plastics and prevent spoilage and microbial contamination of fruits and vegetables during storage, as well as acting as a carrier of functional compounds such as antimicrobials, antioxidants, flavorings, and colors [5, 6]. Additionally, fruit and vegetable puree has been widely used as a biopolymer source to produce edible films [7].

According to the previous studies, different fruit purees, such as apple [8], banana [9], mango [10], and carrot purees [11], were successfully utilized to develop edible films. Since the land dedicated to fruit and vegetable as a biopolymer source for the production of food packaging is negligible, the use of bio-based and biodegradable raw materials with no land uses is essential [12]. In this respect, wastes from food plants are the best source to produce biopolymers due to their low cost and

✉ Ainaz Alizadeh
a.alizadeh@iaut.ac.ir

[1] Department of Food Science and Technology, Tabriz Branch, Islamic Azad University, Tabriz, Iran

[2] Drug Applied Research Center, Tabriz University of Medical Sciences, Tabriz, Iran

[3] Department of Food Science and Technology, Faculty of Agriculture, Urmia University, Urmia, Iran

vast availability [13]. Accordingly, orange production is estimated at 85 million tons annually, and its industrial processing, such as orange juice production, results in 50–60% waste of the raw material [14]. Orange waste has a considerable amount of soluble solids, water, and pH 3–4, causing serious environmental problems when maintenance is improperly [2]. Moreover, it contains pectin, soluble sugars, hemicellulose, cellulose, starch, protein, lignin, ash, fat, and flavonoids, indicating the importance of its recycling process [12]. In this respect, a recent survey on lemon waste has shown successful results for film formation [2]. However, previous studies also have revealed that low molecular weight compounds in fruit and vegetable puree prevent the formation of a continuous film network [15].

Nano-based filler compounds, including nanoclay, nanometals, and cellulose nanofibers, were utilized to improve the physical, mechanical, and gas inhibitory properties of edible films [16, 17]. Cellulose nanofiber is one of the nanoparticles proposed as a reinforcement agent in recent years. They have high chemical and thermal stability compared to other organic nanoparticles. They are further used to improve mechanical strength, thermal resistance, inhibition against gases, transparency, water barrier properties, and film appearance [4, 6, 15]. Moreover, cellulose nanofiber triggers a controlled release of active compounds, as well as the formation of a complex diffusion pathway due to the impermeability of nanofillers [16]. Accordingly, packaging films can also act as carriers of antioxidant, antimicrobial, and active compounds to control pathogens and improve the quality and shelf life of food [18]. Nettle (*Urtica dioica* L.) essential oil, which belongs to the nettle family, is widely known as a medicinal plant and food additive. Nettle has a vast nutritional value, and its high antimicrobial properties are related to carvacrol, which has significant antibacterial, antiviral, antifungal, and antiparasitic effects [19].

Thus far, only a few studies have been conducted about the feasibility of orange waste as the biopolymer base for the production of biodegradable film samples [12, 13, 20]. However, to the best of our knowledge, no previous studies have been performed on preparing a bioactive film from orange waste combined with other reinforcing materials or active agents.

Therefore, the present study aims to evaluate the feasibility of producing nano biocomposite film based on orange juice processing waste containing cellulose nanofiber and nettle essential oil. Further, it investigates the effect of different concentrations of CNF and NEO on the physical, structural, and antimicrobial characteristics of OWP-based nano biocomposite film by FE-SEM, FTIR, XRD, and DSC. Finally, WVP, as well as mechanical and antimicrobial properties of the films, is studied.

Materials and Methods

Materials

Oranges waste (obtained from orange juice production) was procured from Takdaneh Industry Co. (Marand, Iran). Nettle essential oil (NEO) was purchased from Tabibdaru Industry Co. (Kashan, Iran). Calcium sulfate, magnesium nitrate, potassium sulfate, citric acid (monohydrate, > 99.5), and glycerol were obtained from Merck Co. (Darmstadt, Germany). CNF (with an average diameter and length of about 35 nm and 5 µm, respectively, and purity of 99 g/100 g) was procured from Nano Novin Polymer Co. (Saari, Iran). *Listeria monocytogenes* (PTCC 1298), *Salmonella enterica* (PTCC CiP104115), *Pseudomonas aeruginosa* (PTCC 1310), *Staphylococcus aureus* (PTCC 1764), and *Escherichia coli* (PTCC 1163) were prepared from Persian Type Culture Collection (PTCC) (Tehran, Iran). Muller-Hinton agar for the microbiological test was obtained from Sigma-Aldrich (St. Louis, USA).

Preparation of Orange Waste Powder (OWP)

Orange waste obtained from juice extraction was processed according to the method described by Batori et al. (2017) with some modifications [12]. Briefly, orange waste was first washed with water to remove dissolved sugars. For this purpose, orange waste was soaked in water for 24 h. Consequently, two further washing steps were applied and each step consisted of stirring (at 115 rpm) the orange waste immersed in the water bath at 35 °C for 20 min. The ratio of water to orange waste was 1.5:1 in all stages. After draining, the orange waste was collected and dried in the oven (UF 55, Memmert, Germany) at 40 °C for 16 h. Consequently, the dried waste was finely milled and used to prepare the film samples.

Preparation of Nanobiocomposite OWP Based Films

The OWP-based nanobiocomposite film samples were prepared according to the methods of Batori et al., (2017) with some modifications and were coded as Table 1. The film solutions were prepared by incorporating OWP (6% w/v) and CNF (3 and 6% w/w based on OWP weight) in an acidic aqueous solution. The mentioned acidic solution was prepared with 1% (w/v) citric acid and 7% (w/w based on solution weight) glycerol as a plasticizer. Additionally, sonication (UP200H, Hielscher, Teltow, Germany) was utilized (frequency of 40 kHz for 10 min) before the inclusion of CNF solution to obtain a homogeneous and uniform dispersion of CNF particles with less aggregation. Afterward,

Table 1 The fabricated orange waste-based bioactive film samples

Samples	OWP (% w/v)	CNF (% w/v)	NEO (% w/v)
OWP/CNF 0%/NEO 0%	6	–	–
OWP/CNF 0%/NEO 1.5%	6	–	1.5
OWP/CNF 0%/NEO 3%	6	–	3
OWP/CNF 3%/NEO 0%	6	3	-
OWP/CNF 3%/NEO 1.5%	6	3	1.5
OWP/CNF 3%/NEO 3%	6	3	3
OWP/CNF 6%/NEO 0%	6	6	–
OWP/CNF 6%/NEO 1.5%	6	6	1.5
OWP/CNF 6%/NEO 3%	6	6	3

OWP orange waste powder, *CNF* cellulose nanofiber, *NEO* Nettle essential oil

the prepared suspension was blended by using a magnetic stirrer at 115 rpm for 30 min in a water bath at 70 °C and then filtered to remove the large particles. Nettle essential oil (NEO) (1.5 and 3% w/w based on OWP weight), as an antimicrobial agent, was incorporated in the filtered solution after the temperature of film solutions was reduced to room temperature.

Consequently, the prepared solution was homogenized (IKA T25-Digital Ultra Turrax, Staufren, Germany) at 13,500 rpm for 3 min and treated by ultrasound at 40 kHz for 20 min to eliminate the dissolved and undesired air bubbles (degassing operation). Furthermore, OWP-based film without CNF and essential oil incorporation was produced as a control sample for later analyses. Finally, the solutions were cast on the polystyrene plates and dried at 35 °C for 36 h. Moreover, obtained film samples were conditioned in a desiccator with 53% relative humidity (RH) by using saturated magnesium nitrate solution at 25 °C for 36 h [12].

Characterization of Films

Fourier Transforms Infrared (FT-IR)

FT-IR spectroscopy (Tensor27, Bruker, Etlingen, Germany) was used to study the structural interactions of nanocomposite film samples. The spectra were obtained at the wavenumber range of 4000–400 cm^{-1} with a resolution of 4 cm^{-1}. The samples were prepared according to the KBr-pellet method.

Field Emission Scanning Electron Microscopy (FE-SEM)

The surface and cross-sectional surface of the film samples were morphologically studied using FE-SEM (Sigma VP, Zeiss, Obercochen, Germany) after the gold coating of the samples (DST1, nanostructured coating, Tehran, Iran).

X-Ray Diffraction (XRD) Analyses

The x-ray diffractometer (Model Kristalloflex D500, Siemens, Munchen, Germany) in the diffraction angles (2θ) of 5–40° at room temperature was used to obtain the XRD images. To analyze the XRD spectra a Cu Kα radiation source (k = 0.154 nm, 40 kV and 40 mA) was used.

Differential Scanning Calorimetry (DSC)

The thermal properties of film samples were evaluated using the DSC test (DSC400 SANAF, Tehran, Iran). In brief, 20 ± 5 mg of each sample was weighed in the sample pan and an empty pan was considered as a reference. The operation was performed in − 100 to 250 °C at a rate of 10 °C/min to determine the glass transition temperature (T_g) and melting temperature (T_m) of the samples.

Mechanical Properties

In order to study the mechanical properties of film samples, a Tensile Analyzer (DBBP-20, Bongshin, Seongnam, Korea) was used. The film samples were cut in the form of dumbbells (8 cm × 0.5 cm) and mounted in two grips at 50 mm. A 10 mm/min crosshead speed was considered. The mechanical parameters of the samples including elongation to break (ETB) and ultimate tensile strength (UTS) were determined [4].

Water Vapor Permeability (WVP)

To determine the water vapor permeability of the film samples the ASTM E96-05 standard method was used (ASTM, 2005). Film samples were sealed in glass vials with 0% RH and placed in a desiccator with 97% RH at 25 °C. The vials were weighed every 24 h. The changes in weight were recorded versus time and the slope was calculated by linear regression. The water vapor transmission rate (WVTR) was defined as the slope of the linear part of the curve (g/h) divided by the transfer area (m^2). Finally, after sealing the film samples in glass vials containing $CaSO_4$ to reach the vials inside RH to 0%, they were placed in a desiccator containing K_2SO_4 solution to maintain the RH of 97% at 25 °C. The weight of the vials was checked every 24 h. Curves of weight changes versus time were plotted and the slope was determined using linear regression. The water vapor transmission rate (WVTR) was calculated by dividing the slope of the linear part of the curve (grams per hour) by the transfer area (m^2) and the WVP ($\times 10^{-7}$ gPa^{-1} h^{-1} m^{-1}) of film samples was calculated as follows:

$$WVP = \frac{WVTR \times X}{P(R_1 - R_2)} \quad (1)$$

So that, P shows the saturation vapor pressure of water (Pa) at 25 °C, R_1 is the desiccator RH, R_2 is the vial RH and X indicates the film average thickness (m).

Antibacterial Activity

The antimicrobial effect of the film samples on some food-borne pathogenic bacteria, *L. monocytogenes*, *S. enterica*, *P. aeruginosa*, *S. aureus*, and *E. coli* was investigated according to the agar disc diffusion method. In this regard, an active culture of each bacterium was obtained by inoculating single colonies into BHI (brain heart infusion) broth at 37 °C for 24 h. Subsequent dilutions of the stock cultures were made in physiology serum to obtain approximately 1.5×10^8 CFU/mL regarding the 0.5 McFarland standard turbidity test [21]. After preparing suspensions of bacteria they were cultured on the Muller-Hinton agar medium. Film samples were prepared in round shapes with a diameter of 7 mm and placed on the surface of Muller-Hinton agar plates and incubated at 37 °C for 24 h. A caliper was used to determine the inhibition zone around the film sample and the mean values were reported [2].

Statistical Analysis

The statistical evaluation of the data was conducted using a one-way analysis of variance (ANOVA) using IBM SPSS Statistics 26 (IBM Corporation, Armonk, NY, USA). To determine the significant differences among the treatment means, Duncan's multiple test range ($p < 0.05$) was used. All the analyses were performed in three replicates and data presented as mean ± SD.

Results and Discussion

Fourier Transforms Infrared (FT-IR) Spectroscopy

Figure 1 shows the FT-IR spectrum of OWP/CNF0%/NEO0%, OWP/CNF6%/NEO0%, OWP/CNF0%/NEO3%, and OWP/CNF6%/NEO3% film samples. The spectrum of OWP/CNF0%/NEO0% film sample showed several specified peaks summarized as follows: (1) Peaks ranging from 3117 to 3842 cm^{-1} indicated intermolecular O–H stretching vibration bonds of the pectin monomer, besides the symmetric and asymmetric stretching vibration associated with H_2O [7] and free N–H groups of proteins [4]. (2) The peaks around 2822–2885 cm^{-1} were associated with C–H bonds of the methylene group in the polymer structure and stretching vibrations of the methyl group of galacturonic acid methyl ester [5, 22]. (3) The peaks ranging from 1883 to 1990 cm^{-1}

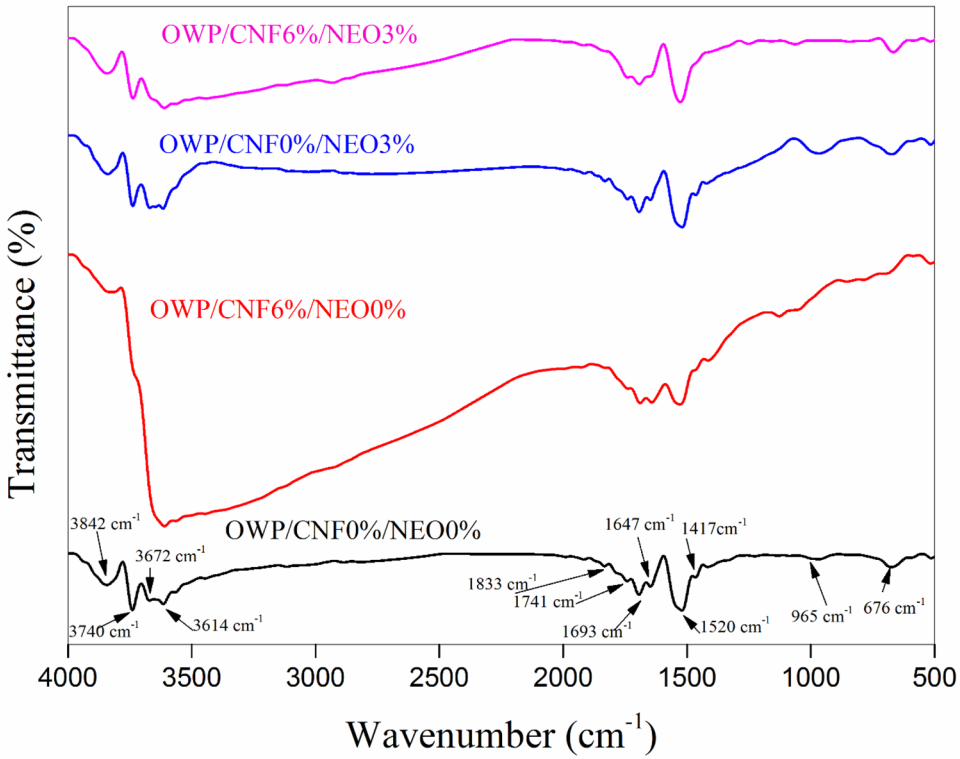

Fig. 1 Fourier transforms infrared (FT-IR) spectra of OWP/CNF0%/NEO0%, OWP/CNF0%/NEO3%, OWP/CNF6%/NEO0 and OWP/CNF6%/NEO3% nanobiocomposite film samples. *OWP* orange waste powder, *CNF* cellulose nanofiber, *NEO* nettle essential oil

belonged to the C–H groups of aromatic compounds. (4) The peaks at 1741 cm^{-1} belonged to the C=O groups of the ester bands [5, 22], possibly related to carbonyl esters [23] or phenolic esters groups, due to the existence of the orange natural essential oil in OWP. (5) The peaks ranging from 1647 to 1693 cm^{-1} associated with the symmetric carboxylate and the non-esterified carbonyl groups in galacturonic acid structure [5, 7, 22]. (6) The peak at 1520 cm^{-1} represented the amide II bands associated with bending vibrations of the N–H groups and stretching vibration of the C–N groups [7]. (7) Absorption bands at 1465, 1417, and 1227 cm^{-1} were associated with the aliphatic chain bending vibrations [7], asymmetric carboxyl vibrations [22], and carboxylic acid stretching vibration of C–O groups in pectin, respectively [5]. (8) The peak at 965 cm^{-1} belonged to the C–O bending vibrations of the pectin structure [24]. (9) Peaks ranging from 500 to 850 cm^{-1} indicated the glycerol adsorption bands [21]. According to the result, the addition of 6% CNF led to disappearing the peaks in the range of 2822–2885, 1883–1990, 1741, 1465, and 417 cm^{-1}, as well as transferring the peak around 1227 and 3117–3842 cm^{-1} to 1126 and 3610–3810 cm^{-1} wavenumbers, showing the strong interactions between film components and CNF. The obtained results were in line with previous studies [4, 22, 25]. Additionally, no new peaks were observed by incorporating 3% NEO into the OWP-based film samples. However, the intensities of the peaks increased compared to the control film due to the limited interactions, as well as increasing free functional groups owing to NEO in the polymer matrix [22]. According to the results, incorporation of 6% CNF and 3% NEO into the OWP-based film sample led to a shift in the peaks wavenumber, disappearance of the peaks around 3117–3300 cm^{-1} due to the formation of strong hydrogen bonds between the film components, NEO, and CNF, and thus reducing free OH groups.

Field Emission-Scanning Electron Microscopy (FE-SEM)

The microstructure of OWP-based film samples with different concentrations of CNF and NEO was studied (Fig. 2). The surface micrograph displayed a heterogeneous and rough structure of the films prepared from OWP, which was common in films produced from more than one component, such as films made from fruit puree due to the existence of complex soluble and insoluble compounds [12]. However, the incorporation of 6% CNF into the OWP-based film matrix led to a dense sheet-like structure in the films due to the uniform distribution of CNF in the film matrix and the strong interaction of CNF with pectin chains. The results were in line with previous studies [26, 27]. According to the micrographs, the inclusion of 3% NEO to OWP-based film could change the matrix structure and create a rough and spongy surface. In this respect, cross-sectional images also showed a rough structure with small cavities in some parts of the films containing NEO. This phenomenon could be due to the volatility of the essential oil present in the film matrix that created the porosity during the drying process. Similar results have been obtained by other researchers [1, 3]. However, Kamkar et al. (2021) characterized a nearly smooth surface morphology and homogenous structure with a good dispersion for chitosan biopolymer loaded with nano-liposomal essential oil [28]. Based on the results, the inclusion of 6% CNF and 3% NEO could eliminate the adverse effect of NEO by forming strong bonds between the NEO and CNF to prevent the migration of essential oil to the surface during the drying period.

X-Ray Diffraction (XRD) Analyses

Figure 3 illustrates the XRD diffractions of OWP/CNF0%/NEO0%, OWP/CNF6%/NEO0%, OWP/CNF0%/NEO3%, and OWP/CNF6%/NEO3% film samples. The diffractogram of the OWP/CNF0%/NEO0% film sample showed three main peaks at 2θ of 12°, 15°, and 20°, indicating the semi-crystalline structure of the OWP-based film sample [29]. As mentioned, the main compound of OWP was pectin, and the peaks at 2θ of 12.72°, 16.30°, 18.45°, 25.32°, and 40° were reported to be associated with the pure pectin crystallinity [22]. Additionally, pure CNF showed a diffraction pattern with three specific peaks at 2θ of 14.54°, 16.92°, and 22.72°. The diffraction profiles of spectrum pertaining to the OWP/CNF6%/NEO0% showed that the addition of CNF resulted in the removal of the peak at 2θ of 15° and the appearance of a new peak at 2θ of 37°. In contrast, the control film indicated a uniform distribution without CNF agglomeration in the film matrix, indicating good compatibility of CNF and pectin and forming new crystalline regions in amorphous areas [22, 30]. These results were in line with the findings of other authors [22, 31]. However, Soofi et al. (2021) reported the improper dispersion of rigid CNF at high concentrations between the lemon waste bases polymer chains, leading to the CNF agglomeration in the film structure and being shown by the appearance of pure CNF specific peak in lower intensities in diffractogram [2].

In the light of the results, the OWP-based film sample containing NEO showed just one peak near 2θ of 12° due to NEO in the matrix that increased the mobility of the polymer chain and limited the formation of a crystalline structure (Zhang et al., 2020). However, the diffractogram of OWP/CNF6%/NEO3% film sample revealed two peaks near 2θ of 12° and 14° due to CNF in the film matrix that limited the mobility of polymer chains caused by incorporating NEO.

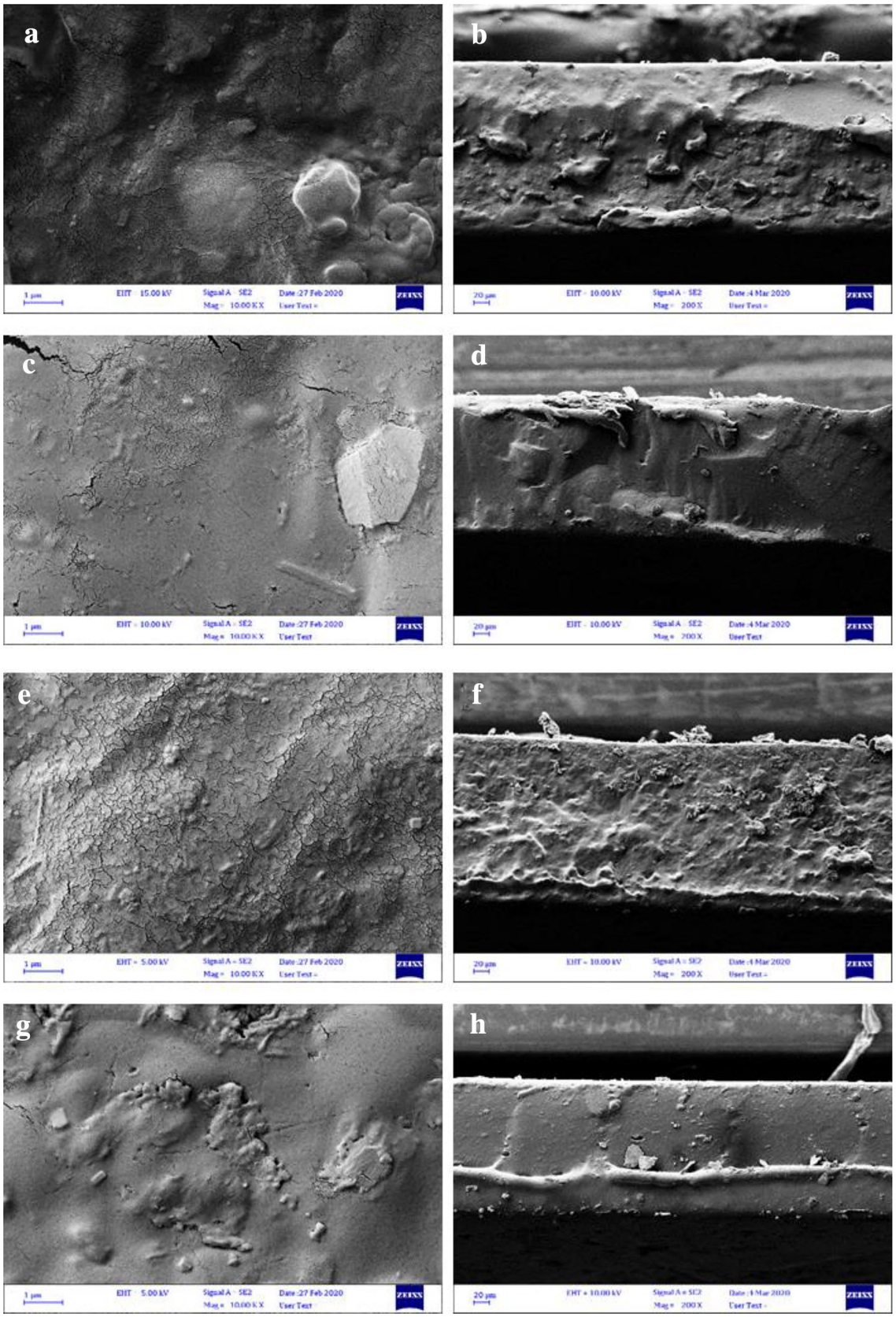
a
b
c
d
e
f
g
h

◂**Fig. 2** Field emission scanning electron microscopy (FE-SEM) images of surface and cross section of OWP/CNF0%/NEO0% (**a** and **b**), OWP/CNF6%/NEO0% (**c** and **d**), OWP/CNF0%/NEO3% (**e** and **f**) and OWP/CNF6%/NEO3% (**g** and **h**) nanobiocomposite film samples *OWP* orange waste powder, *CNF* cellulose nanofiber, *NEO* nettle essential oil

Differential Scanning Calorimetry (DSC)

Table 2 presents the thermal properties of OWP-based nanocomposites. According to the results, the T_g value and melting temperature of the OWP/CNF0%/NEO0% film sample were − 87.9 °C and 125.7 °C, respectively. The low T_g value in OWP-based film samples was related to the polymer structure and its internal properties and hydrophilic nature. Accordingly, water molecules also caused the mobility of polymer chains, leading to a reduction in T_g value due to their lubricating and quasi-plasticizing characteristics. Moreover, other soluble solid compounds in orange waste, such as sugar, with plasticizing effects, led to a decrease in the T_g value of these films compared to those prepared from pure pectin. The sub-zero T_g value of the produced OWP-based films indicated relatively poor chemical stability due to high molecular mobility and thus high reactivity of the film components. However, the low T_g of these films implies optimal flexibility at refrigerator temperatures [22]. Based on the results, the incorporation of 6% CNF increased the T_g and T_m values of OWP-based films to − 86.6 °C and 152.9 °C, respectively, possibly due to the interactions between pectin and CNF and increased film crystallinity. Additionally, the inclusion of CNF in the biopolymer matrix increases the formation of heterogeneous nuclei and facilitates crystallization [32], as well as reducing the free space between the chains and decreasing mobility. Furthermore, the interactions of CNF with water molecules led to their redistribution in the biopolymer matrix and reduced the plasticizing effects of water molecules while consequently increasing the T_g value. Also, the migration of glycerol from polymer-rich to CNF containing regions could reduce the plasticizing effect of glycerol [33]. Similar results were obtained by other authors [15, 34].

According to the thermographs, the addition of 3% NEO decreased T_g and increased T_m values to − 98.9 and 158.0 °C, respectively, compared to the control sample. The single glass transition temperature that appeared in the thermograph indicated the uniform distribution of NEO molecules in the biopolymer matrix. Furthermore, the plasticizing effect of the NEO increased the mobility of polymer chains in the amorphous region, leading to shifted T_g value of the film to lower temperatures. This phenomenon revealed that NEO-polymer bonds were weaker than those of polymer–polymer, leading to increased mobility of polymer chains at lower temperatures [35]. On the other hand, the increased melting point of NEO-containing samples was due to the high molecular weight and lipophilic nature of essential oil, which were in line with the previous studies [3, 36, 37]. Results also showed a slight increase in the T_g (− 87.7 °C) and T_m (126.1 °C) values, compared to the control film, by adding NEO and CNF, which was due to the interactions between CNF and NEO. This resulted in the reduced plasticizing effect of essential oil and limited mobility of biopolymer chains by increasing structural cohesion and thus the T_g value of this film.

Mechanical Properties

The evaluated mechanical properties of OWP-based film samples containing different concentrations of CNF and NEO are summarized in Table 3. Referring to the obtained results, by increasing the concentration of CNF from 0 to 6%, the UTS values of the film samples increased (from 4.88 ± 0.10 to 7.66 ± 0.29 MPa), and the % E value decreased (from 32.40 ± 0.36 to 20.94 ± 0.81%) significantly ($p < 0.05$). This phenomenon could be due to the uniform distribution of CNF in the film matrix and the formation of high interactions between CNF and pectin, reducing the relative mobility of polymer chains and resulting in stiffer films with less flexibility [38, 39].

Additionally, natural strength and rigidity of CNF [2], high density of nanomaterials compared to biopolymer matrix, filling free spaces in amorphous domains, creating a strong network as a result of increased hydrogen bonds, and increasing the crystalline regions of the matrix were the other factors that enhanced the mechanical properties of the CNF incorporated film samples, which were in accordance with previous studies [5, 22, 32].

As found, the mechanical strength of NEO incorporated films decreases significantly ($p < 0.05$) compared to the control sample. This phenomenon could be due to the formation of weak biopolymer-NEO interactions compared with those of strong biopolymer-biopolymer [40].

Furthermore, increasing the concentration of NEO from 1.5 to 3% decreases the UTS values of the film samples from 4.38 ± 0.18 to 3.78 ± 0.18 MPa, which could be due to (1) a change in the uniformity of the film network, (2) the reduction in intermolecular interactions of pectin, and (3) the formation of microcavities due to entrapment of oil droplets in the continuous polymer matrix [36]. Also, increasing the flexibility and the % E value of film samples by incorporating NEO could be related to the plasticizing effects of the essential oil due to the reduced intermolecular interactions and increased ductile properties [41]. Accordingly, the liquid form of essential oil at room temperature also facilitates the film deformation and increases the E% value of the films [42]; similar results have been reported by other researchers [40, 43]. Obtained results

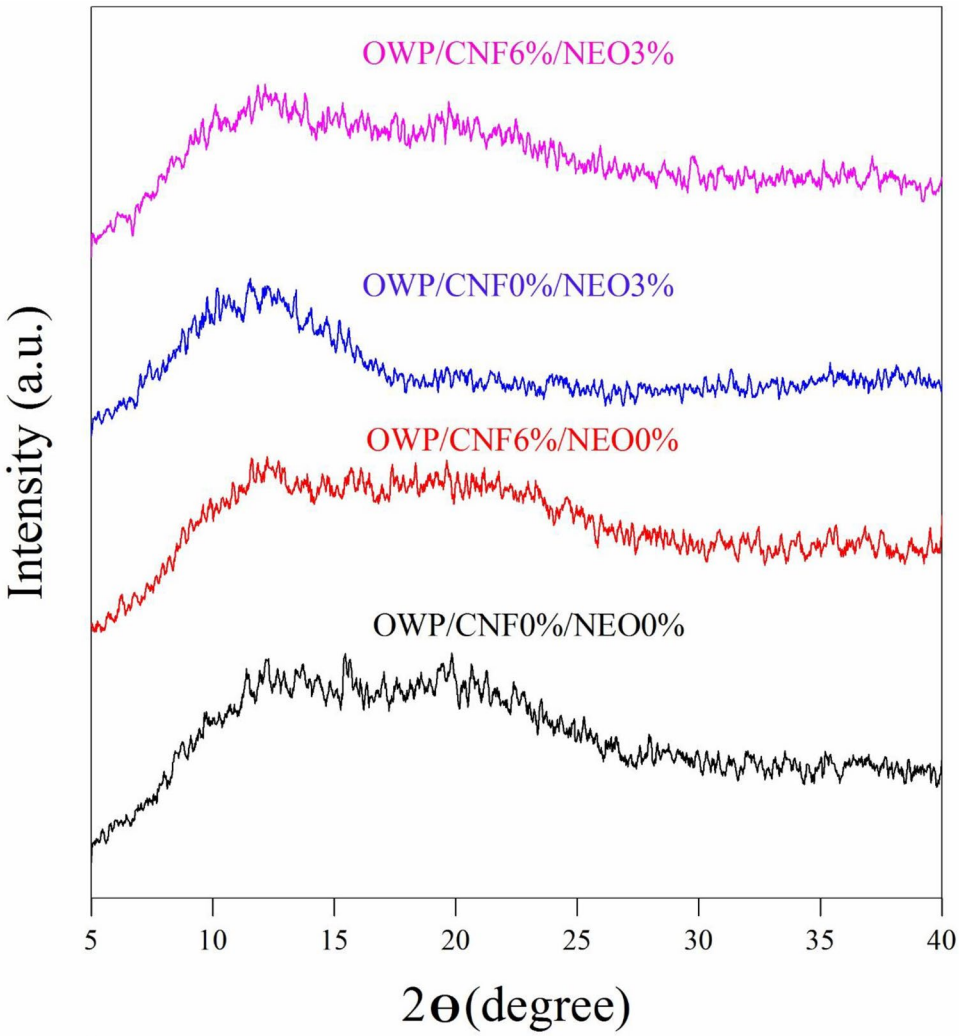

Fig. 3 X-ray diffraction (XRD) patterns OWP/CNF0%/NEO0%, OWP/CNF0%/NEO3%, OWP/CNF6%/NEO0% and OWP/CNF6%/NEO3% nanobiocomposite film samples. *OWP* orange waste powder, *CNF* cellulose nanofiber, *NEO* nettle essential oil

Table 2 Thermal properties of orange waste-based bioactive film samples

Samples	T_g (°C)	T_m (°C)
OWP/CNF 0%/NEO 0%	− 87.9	125.7
OWP/CNF 6%/NEO 0%	− 86.6	152.9
OWP/CNF 0%/NEO 3%	− 98.9	158.0
OWP/CNF 6%/NEO 3%	− 87.7	126.1

OWP orange waste powder, *CNF* cellulose nanofiber, *NEO* Nettle essential oil, T_g glass transition temperature, T_m melting temperature

also revealed that the incorporation of CNF and NEO in combination improved the mechanical properties of film samples compared to the control film. Increased UTS and decreased % E values in this sample could be explained by CNF-NEO interactions able to eliminate the negative effect of NEO on reducing cross-chain interactions. Remarkably, the findings were also in line with the SEM and FTIR results.

Water Vapor Permeability

The WVP values of the film samples are summarized in Table 3. The results showed a significant effect ($p < 0.05$) of the additives on water vapor permeability. Accordingly, as the concentration of CNF increased from 3 to 6%, the WVP values of the films decreased from $3.13 \pm 0.12 \times 10^{-7}$ to $1.02 \pm 0.07 \times 10^{-7}$ gPa^{-1} h^{-1} m^{-1}, which may be related to (1) the reduction in hydrogen bonds in the film due to electrostatic interactions between CNF and pectin hydroxyl groups that decreased the water possibility to interact with free active groups, (2) the CNF structure and its possibility to form intermolecular bonds in a biopolymer, (3) compatibility of CNF with polysaccharide biopolymers and consequently greater affinity to create a continuous network in the biopolymer matrix, (4) the reduction in free spaces in the film matrix due to the pectin-CNF interactions, and (5) the uniform distribution of CNF in the film matrix resulting in zigzag and tortuous paths for the penetration of water vapor molecules. These results were in line with the findings

Table 3 WVP and mechanical properties orange waste-based bioactive film samples

Samples	UTS (MPa)	EB (%)	WVP ($\times 10^{-7}$ gPa^{-1} h^{-1} m^{-1})
OWP/CNF 0%/NEO 0%	4.88 ± 0.10^{g}	32.40 ± 0.36^{c}	3.13 ± 0.12^{c}
OWP/CNF 0%/NEO 1.5%	4.38 ± 0.18^{h}	34.03 ± 0.75^{b}	3.35 ± 0.07^{b}
OWP/CNF 0%/NEO 3%	3.78 ± 0.18^{i}	36.09 ± 0.61^{a}	3.66 ± 0.09^{a}
OWP/CNF 3%/NEO 0%	6.20 ± 0.10^{d}	27.81 ± 0.55^{f}	2.18 ± 0.17^{f}
OWP/CNF 3%/NEO 1.5%	5.86 ± 0.23^{e}	29.51 ± 0.69^{e}	2.47 ± 0.09^{e}
OWP/CNF 3%/NEO 3%	5.38 ± 0.21^{f}	31.31 ± 0.34^{d}	2.85 ± 0.14^{d}
OWP/CNF 6%/NEO 0%	7.66 ± 0.29^{a}	20.94 ± 0.81^{i}	1.02 ± 0.07^{i}
OWP/CNF 6%/NEO 1.5%	7.35 ± 0.10^{b}	22.79 ± 0.43^{h}	1.37 ± 0.12^{h}
OWP/CNF 6%/NEO 3%	6.75 ± 0.08^{c}	24.75 ± 0.50^{g}	1.68 ± 0.10^{g}

Data are expressed as mean ± standard deviation (n = 3) and different letters show significant difference at the 5% level in Duncan's test ($p < 0.05$)

OWP orange waste powder, *CNF* cellulose nanofiber, *NEO* nettle essential oil, *EB* elongation at break, *UTS* ultimate tensile strength

of other researchers [5, 22]. As found, by increasing the concentration of NEO (1.5–3%), the WVP values of the film samples increased significantly ($3.13 \pm 0.12 \times 10^{-7}$ to $3.66 \pm 0.09 \times 10^{-7}$ gPa^{-1} h^{-1} m^{-1}) due to the destruction of the film matrix and formation of cracks and cavities in the films, consistent with the SEM analyses.

Furthermore, essential oils are liquid at room temperature; they can easily be deformed in the film structure and cause the flexibility and mobility of molecular chains, resulting in better permeability of water molecules through the film [22]. Moreover, high WVP values in the NEO incorporated films could be due to the negative effect of NEO on the pectin intermolecular bonds, as well as the formation of micro-cavities in film structure due to the evaporation of essential oils during drying [44]. Crystallization was another central factor affecting the WVP of biopolymers. However, obtained results were inconsistent with findings of Nisar et al. (2018) that reported a decrease in WVP values by incorporation of clove bud essential oil into citrus pectin film due to its hygroscopic characteristics [22].

Accordingly, more crystalline polymers are less permeable to water vapor due to the continuous structure [2], in line with the XRD and DSC results that showed the reduction in crystallization and increase in the WVP value of the OWP-based film samples by incorporating NEO. Although the hydrophobicity of essential oils affects the films' WVP, the physical factors are more effective on the permeability of water vapor in the films. It cannot be assumed that the WVP of films is easily reduced by adding a hydrophobic component to the film formulation [45], as found in other studies [1, 3, 44]. Results also showed that barrier properties of film samples containing CNF and NEO in combination improved compared to control and individual NEO incorporated film samples. Further, CNF-NEO interactions increased crystallization, as well as decreasing free spaces and free hydroxyl groups in the film matrix, resulting in lower hydrophilicity of the films.

Antibacterial Activity

The antibacterial activity of the prepared film samples is presented in Table 4. According to the results, the control film had a significant inhibitory effect against both Gram-positive (*L. monocytogenes* and *S. aureus*) and Gram-negative bacteria (*P. aeruginosa, E. coli, and S. enterica*) due to the low pH of the prepared films and the existence of natural antimicrobial compounds such as orange essential oil in OWP. The orange essential oil contains terpenes, sesquiterpenes, aldehydes, alcohols, esters, hydrocarbons, and oxygenated compounds with antioxidant and antimicrobial properties [20, 46].

Further, the obtained results showed Gram-positive bacteria to be more sensitive to the film's natural antimicrobial compounds than Gram-negative bacteria due to differences in cell wall structures. Peptidoglycans and small proteins are the major components of the cell wall in Gram-positive bacteria. However, the cell wall of Gram-negative bacteria is more complex; it contains various polysaccharides, proteins, lipids, peptidoglycan, as well as an outer membrane that covers the cell wall surface, making it difficult for the active compound to permeate through the cell wall [40]. The present research results were in line with those of previous studies [2, 40].

The results revealed that NEO-containing film samples exhibited antibacterial activity against all tested bacteria; also, the antimicrobial activity of the films enhanced significantly ($p < 0.05$) with increasing the NEO concentration. The highest antibacterial activity was observed in the OWP/CNF 6%/NEO 3% film sample with inhibition zones of 20.66 ± 0.57, 21.66 ± 1.52, 14.33 ± 0.57, 11.66 ± 0.57, and 11.65 ± 1.52 mm against *S. aureus*, *L. monocytogenes*, *E. coli*, *S. enterica*, and *P. aeruginosa*, respectively; these results were similar to those obtained by other researchers [40, 47, 48].

According to the results, *E. coli*, *L. monocytogenes*, *S. aureus,* and *P. aeruginosa* were the most sensitive bacterial species, respectively, and *S. enterica* was the most resistant to NEO. The antimicrobial activity of nettle essential oil was related to phenol, 2-methyl-5-(1-methyl ethyl), or

Table 4 Inhibition zones produced by different film types on tested bacteria

Samples	Inhibition zone (mm) of films Tested bacteria				
	S. aureus	*L. monocytogenes*	*E. coli*	*S. enterica*	*P. aeroginosa*
OWP/CNF 0%/NEO 0%	10.33 ± 1.52^{c}	10.33 ± 1.15^{c}	ND	7.33 ± 0.57^{c}	3.00 ± 1.41^{c}
OWP/CNF 0%/NEO 1.5%	16.00 ± 2.00^{b}	16.33 ± 0.57^{b}	7.66 ± 1.52^{b}	9.66 ± 0.57^{b}	7.33 ± 0.57^{b}
OWP/CNF 0%/NEO 3%	20.66 ± 0.57^{a}	21.66 ± 1.52^{a}	14.33 ± 0.57^{a}	11.66 ± 0.57^{a}	11.66 ± 1.52^{a}
OWP/CNF 3%/NEO 0%	10.66 ± 1.52^{c}	10.00 ± 1.00^{c}	ND	7.66 ± 1.15^{c}	3.66 ± 2.08^{c}
OWP/CNF 3%/NEO 1.5%	16.33 ± 1.52^{b}	15.66 ± 1.52^{b}	7.33 ± 2.08^{b}	9.33 ± 0.57^{b}	7.66 ± 1.52^{b}
OWP/CNF 3%/NEO 3%	20.33 ± 2.08^{a}	20.66 ± 2.08^{a}	15.33 ± 2.51^{a}	11.33 ± 0.57^{a}	11.33 ± 0.57^{a}
OWP/CNF 6%/NEO 0%	10.00 ± 1.00^{c}	10.00 ± 2.00^{c}	ND	7.33 ± 1.15^{c}	3.33 ± 1.15^{c}
OWP/CNF 6%/NEO 1.5%	16.33 ± 2.08^{b}	16.66 ± 1.52^{b}	8.00 ± 2.64^{b}	9.33 ± 0.57^{b}	8.00 ± 1.00^{b}
OWP/CNF 6%/NEO 3%	21.33 ± 0.57^{a}	22.33 ± 2.51^{a}	15.33 ± 1.15^{a}	11.66 ± 1.52^{a}	11.66 ± 0.57^{a}

Data are expressed as mean ± standard deviation (n = 3) and different letters show significant difference at the 5% level in Duncan's test ($p < 0.05$)
ND not determined, *OWP* orange waste powder, *CNF* cellulose nanofiber, *NEO* nettle essential oil

carvacrol content [19]. Gul et al. (2012) report that carvacrol, as a monoterpenoid phenol, is the major compound of NEO and has a significant antibacterial, antiviral, antifungal, and antiparasitic effect [19]. Carvacrol destroys the outer membrane of microorganisms, causing the release of liposaccharides, increasing the permeability of the cytoplasmic membrane to ATP, and consequently killing cells [2]. Additionally, phenolic compounds of NEO could denaturize bacterial enzymes and get bounded with minerals, vitamins, and carbohydrates to keep them out of the reach of microorganisms [2].

Conclusion

Cellulose nanofiber and nettle essential oil in different concentrations were successfully used to prepare active nano biocomposite film based on orange waste for the first time. The results showed the compatibility between CNF and NEO with OWP compounds. Moreover, significantly reduced water vapor permeability and %E values, as well as increased tensile strength, in film samples were observed due to an increase in the CNF amount. Compared to the control film, the inclusion of NEO at a concentration of 3% caused a maximum reduction in tensile strength and an increase in melting temperature and water vapor permeability values. The SEM results confirmed uniform distribution, improved structure of film samples by the inclusion of CNF, and the effect of NEO in the formation of porous structure in film samples. Moreover, films containing CNF and NEO had acceptable thermal and crystalline properties. The T_g was increased to higher temperatures, and the thermal stability was reduced by incorporating 6% CNF and 3% NEO in combination. The obtained results also showed that the OWP film samples had an acceptable antimicrobial effect against five foodborne pathogen bacteria; therefore, the addition of NEO increased the antimicrobial properties of film samples. In this regard, the maximum and minimum susceptibility was related to the *S. aureus* and *S. enterica*, respectively. In conclusion, orange juice processing waste is a promising compound for preparing biodegradable bioactive films with improved physical, structural, and microbial properties by incorporating CNF and NEO. However, further investigations are needed to examine the performance of the film on different food systems to replace non-biodegradable plastics.

Acknowledgements The authors gratefully acknowledge the supports of the Islamic Azad University, Tabriz Branch. This research did not receive any specific grant from funding agencies in the public, commercial, or not-for-profit sectors.

References

1. Dashipour A, Razavilar V, Hosseini H et al (2015) Antioxidant and antimicrobial carboxymethyl cellulose films containing *Zataria multiflora* essential oil. Int J Biol Macromol 72:606–613. https://doi.org/10.1016/j.ijbiomac.2014.09.006
2. Soofi M, Alizadeh A, Hamishehkar H et al (2021) Preparation of nanobiocomposite film based on lemon waste containing cellulose nanofiber and savory essential oil: a new biodegradable active packaging system. Int J Biol Macromol 169:352–361. https://doi.org/10.1016/j.ijbiomac.2020.12.114
3. Jouki M, Yazdi FT, Mortazavi SA, Koocheki A (2014) Quince seed mucilage films incorporated with oregano essential oil: physical, thermal, barrier, antioxidant and antibacterial properties. Food Hydrocoll 36:9–19. https://doi.org/10.1016/j.foodhyd.2013.08.030
4. Karimi N, Alizadeh A, Almasi H, Hanifian S (2020) Preparation and characterization of whey protein isolate/polydextrose-based nanocomposite film incorporated with cellulose nanofiber and *L. plantarum*: a new probiotic active packaging system. LWT. https://doi.org/10.1016/j.lwt.2019.108978
5. Viana RM, Sá NMSM, Barros MO et al (2018) Nanofibrillated bacterial cellulose and pectin edible films added with fruit purees.

Carbohydr Polym 196:27–32. https://doi.org/10.1016/j.carbpol.2018.05.017
6. Zabihollahi N, Alizadeh A, Almasi H et al (2020) Development and characterization of carboxymethyl cellulose based probiotic nanocomposite film containing cellulose nanofiber and inulin for chicken fillet shelf life extension. Int J Biol Macromol 160:409–417
7. Tulamandi S, Rangarajan V, Rizvi SSH et al (2016) A biodegradable and edible packaging film based on papaya puree, gelatin, and defatted soy protein. Food Packag Shelf Life 10:60–71. https://doi.org/10.1016/j.fpsl.2016.10.007
8. Mohebbi M, Ansarifar E, Hasanpour N, Amiryousefi MR (2012) Suitability of *Aloe vera* and gum tragacanth as edible coatings for extending the shelf life of button mushroom. Food Bioprocess Technol 5:3193–3202
9. Razavi SMA, Amini AM, Zahedi Y (2015) Characterisation of a new biodegradable edible film based on sage seed gum: influence of plasticiser type and concentration. Food Hydrocoll 43:290–298
10. Seyedi S, Koocheki A, Mohebbi M, Zahedi Y (2014) *Lepidium perfoliatum* seed gum: a new source of carbohydrate to make a biodegradable film. Carbohydr Polym 101:349–358
11. Wang X, Sun X, Liu H et al (2010) Food and Bioproducts Processing Barrier and mechanical properties of carrot puree films. Food Bioprod Process 89:149–156. https://doi.org/10.1016/j.fbp.2010.03.012
12. Bátori V, Jabbari M, Åkesson D et al (2017) Production of pectin-cellulose biofilms: a new approach for citrus waste recycling. Int J Polym Sci. https://doi.org/10.1155/2017/9732329
13. McKay S, Sawant P, Fehlberg J, Almenar E (2021) Antimicrobial activity of orange juice processing waste in powder form and its suitability to produce antimicrobial packaging. Waste Manag 120:230–239
14. FAO (2018) Food and Agriculture Organization of the United Nations Cropping Database. FAO, Rome
15. Azeredo HMC, Mattoso LHC, Wood D et al (2009) Nanocomposite edible films from mango puree reinforced with cellulose nanofibers. J Food Sci 74:31–35. https://doi.org/10.1111/j.1750-3841.2009.01186.x
16. Oun AA, Rhim JW (2015) Preparation and characterization of sodium carboxymethyl cellulose/cotton linter cellulose nanofibril composite films. Carbohydr Polym 127:101–109. https://doi.org/10.1016/j.carbpol.2015.03.073
17. Sherafatkhah Azari S, Alizadeh A, Roufegarinejad L et al (2020) Preparation and characterization of gelatin/β-glucan nanocomposite film incorporated with ZnO nanoparticles as an active food packaging system. J Polym Environ. https://doi.org/10.1007/s10924-020-01950-1
18. Esmaeili H, Cheraghi N, Khanjari A et al (2020) Incorporation of nanoencapsulated garlic essential oil into edible films: a novel approach for extending shelf life of vacuum-packed sausages. Meat Sci. https://doi.org/10.1016/j.meatsci.2020.108135
19. Gül S, Emirci B, Başer KH et al (2012) Chemical composition and in vitro cytotoxic, genotoxic effects of essential oil from *Urtica dioica* L. Bull Environ Contam Toxicol 88:666–671. https://doi.org/10.1007/s00128-012-0535-9
20. Bassania A, Montesb S, Jubeteb E et al (2019) Incorporation of waste orange peels extracts into PLA films. Chem Eng. https://doi.org/10.3303/CET1974178
21. Ghadetaj A, Almasi H, Mehryar L (2018) Development and characterization of whey protein isolate active films containing nanoemulsions of *Grammosciadium ptrocarpum* Bioss. essential oil. Food Packag Shelf Life 16:31–40. https://doi.org/10.1016/j.fpsl.2018.01.012
22. Nisar T, Wang ZC, Yang X et al (2018) Characterization of citrus pectin films integrated with clove bud essential oil: physical, thermal, barrier, antioxidant and antibacterial properties. Int J Biol Macromol 106:670–680. https://doi.org/10.1016/j.ijbiomac.2017.08.068
23. Šešlija S, Nešić A, Ružić J et al (2018) Edible blend films of pectin and poly(ethylene glycol): preparation and physico-chemical evaluation. Food Hydrocoll 77:494–501. https://doi.org/10.1016/j.foodhyd.2017.10.027
24. Szymanska-Chargot M, Zdunek A (2013) Use of FT-IR spectra and PCA to the bulk characterization of cell wall residues of fruits and vegetables along a fraction process. Food Biophys 8:29–42. https://doi.org/10.1007/s11483-012-9279-7
25. Rajinipriya M, Nagalakshmaiah M, Robert M, Elkoun S (2018) Homogenous and transparent nanocellulosic films from carrot. Ind Crops Prod 118:53–64. https://doi.org/10.1016/j.indcrop.2018.02.076
26. Zykwinska AW, Ralet MCJ, Garnier CD, Thibault JFJ (2005) Evidence for in vitro binding of pectin side chains to cellulose. Plant Physiol 139:397–407. https://doi.org/10.1104/pp.105.065912
27. Shahmohammadi Jebel F, Almasi H (2016) Morphological, physical, antimicrobial and release properties of ZnO nanoparticles-loaded bacterial cellulose films. Carbohydr Polym 149:8–19. https://doi.org/10.1016/j.carbpol.2016.04.089
28. Molaee-Aghaee E, Kamkar A, Akhondzadeh-Basti A, Khanjari A (2021) Antimicrobial effect of garlic essential oil (*Allium sativum* L.) in combination with chitosan biodegradable coating films. Int J Food Microbiol 342:109071
29. Mahardika M, Abral H, Kasim A et al (2019) Properties of cellulose nanofiber/bengkoang starch bionanocomposites: effect of fiber loading. LWT 116:108554
30. Fernandes SCM, Oliveira L, Freire CSR et al (2009) Novel transparent nanocomposite films based on chitosan and bacterial cellulose. Green Chem 11:2023–2029. https://doi.org/10.1039/b919112g
31. Atef M, Rezaei M, Behrooz R (2014) Preparation and characterization agar-based nanocomposite film reinforced by nanocrystalline cellulose. Int J Biol Macromol 70:537–544. https://doi.org/10.1016/j.ijbiomac.2014.07.013
32. Sahraee S, Milani JM, Ghanbarzadeh B, Hamishehkar H (2017) Effect of corn oil on physical, thermal, and antifungal properties of gelatin-based nanocomposite films containing nano chitin. LWT Food Sci Technol 76:33–39. https://doi.org/10.1016/j.lwt.2016.10.028
33. Pelissari FM, Andrade-Mahecha MM, do Sobral PJA, Menegalli FC (2017) Nanocomposites based on banana starch reinforced with cellulose nanofibers isolated from banana peels. J Colloid Interface Sci 505:154–167. https://doi.org/10.1016/j.jcis.2017.05.106
34. Petersson L, Oksman K (2006) Biopolymer based nanocomposites: comparing layered silicates and microcrystalline cellulose as nanoreinforcement. Compos Sci Technol 66:2187–2196. https://doi.org/10.1016/j.compscitech.2005.12.010
35. Ghanbarzadeh B, Almasi H, Entezami AA (2010) Physical properties of edible modified starch/carboxymethyl cellulose films. Innov Food Sci Emerg Technol 11:697–702. https://doi.org/10.1016/j.ifset.2010.06.001
36. Ghanbarzadeh B, Almasi H (2011) Physical properties of edible emulsified films based on carboxymethyl cellulose and oleic acid. Int J Biol Macromol 48:44–49. https://doi.org/10.1016/j.ijbiomac.2010.09.014
37. Ghanbarzadeh B, Oromiehi AR (2009) Thermal and mechanical behavior of laminated protein films. J Food Eng 90:517–524. https://doi.org/10.1016/j.jfoodeng.2008.07.018
38. Huq T, Salmieri S, Khan A et al (2012) Nanocrystalline cellulose (NCC) reinforced alginate based biodegradable nanocomposite film. Carbohydr Polym 90:1757–1763. https://doi.org/10.1016/j.carbpol.2012.07.065

39. Shankar S, Rhim JW (2016) Preparation of nanocellulose from micro-crystalline cellulose: the effect on the performance and properties of agar-based composite films. Carbohydr Polym 135:18–26. https://doi.org/10.1016/j.carbpol.2015.08.082
40. Shojaee-Aliabadi S, Hosseini H, Mohammadifar MA et al (2013) Characterization of antioxidant-antimicrobial κ-carrageenan films containing *Satureja hortensis* essential oil. Int J Biol Macromol 52:116–124. https://doi.org/10.1016/j.ijbiomac.2012.08.026
41. Ramos M, Jiménez A, Peltzer M, Garrigós MC (2012) Characterization and antimicrobial activity studies of polypropylene films with carvacrol and thymol for active packaging. J Food Eng 109:513–519. https://doi.org/10.1016/j.jfoodeng.2011.10.031
42. Fabra MJ, Talens P, Chiralt A (2008) Tensile properties and water vapor permeability of sodium caseinate films containing oleic acid-beeswax mixtures. J Food Eng 85:393–400. https://doi.org/10.1016/j.jfoodeng.2007.07.022
43. Jamróz E, Juszczak L, Kucharek M (2018) Investigation of the physical properties, antioxidant and antimicrobial activity of ternary potato starch-furcellaran-gelatin films incorporated with lavender essential oil. Int J Biol Macromol 114:1094–1101. https://doi.org/10.1016/j.ijbiomac.2018.04.014
44. Ahmad M, Benjakul S, Prodpran T, Agustini TW (2012) Physico-mechanical and antimicrobial properties of gelatin film from the skin of unicorn leatherjacket incorporated with essential oils. Food Hydrocoll 28:189–199. https://doi.org/10.1016/j.foodhyd.2011.12.003
45. Hosseini MH, Razavi SH, Mousavi MA (2009) Antimicrobial, physical and mechanical properties of chitosan-based films incorporated with thyme, clove and cinnamon essential oils. J food Process Preserv 33:727–743
46. Espinosa-Pardo FA, Nakajima VM, Macedo GA et al (2017) Extraction of phenolic compounds from dry and fermented orange pomace using supercritical CO2 and cosolvents. Food Bioprod Process 101:1–10. https://doi.org/10.1016/j.fbp.2016.10.002
47. Hosseini SF, Rezaei M, Zandi M, Farahmandghavi F (2015) Bio-based composite edible films containing *Origanum vulgare* L. essential oil. Ind Crops Prod 67:403–413. https://doi.org/10.1016/j.indcrop.2015.01.062
48. Shojaee-Aliabadi S, Mohammadifar MA, Hosseini H et al (2014) Characterization of nanobiocomposite kappa-carrageenan film with *Zataria multiflora* essential oil and nanoclay. Int J Biol Macromol 69:282–289. https://doi.org/10.1016/j.ijbiomac.2014.05.015